J. Phys. B: At. Mol. Opt. Phys. 24 (1991) 3517–3529. Printed in the UK

R-matrix calculations of vibrationally resolved positron–N_2 scattering cross sections

Grahame Danby† and Jonathan Tennyson‡

† Department of Physics and Astronomy, University of Oklahoma, Norman, OK 73019, USA

‡ Department of Physics and Astronomy, University College London, London WC1E 6BT, UK

Received 24 April 1991

Abstract. The molecular R-matrix method has been used to perform *ab initio* positron–N_2 scattering calculations in the fixed-nuclei approximation. Various treatments of polarization and correlation effects have been studied, including the introduction of up to 22 polarized pseudostates. A model in which the N_2 comprised an SCF ground state and 10 excited pseudostates was adopted for 12 internuclear geometries ranging from 1.6 to 2.9 a_0. Vibrationally elastic and inelastic cross sections are obtained using the adiabatic nuclei approximation and a non-adiabatic model. Non-adiabatic effects are significant for the $v = 0 \rightarrow 1$ cross section (and dominate the small $v = 0 \rightarrow 2$ result). Some early calculations at the equilibrium geometry ($R = 2.068\ a_0$) have been corrected.

1. Introduction

The complicated many-body nature of the short-range interaction between an electron and a molecule has encouraged the development of methods relying on a partitioning of configuration space into short- and long-range parts (Chang and Fano 1972, Morrison 1983). The utility of the molecular R-matrix method derives from the application of quantum chemical electronic structure programs to treat the bound and single continuum electrons within a sphere encasing the target charge cloud. In the outer region the electron–molecule interaction potential is local and may be written in terms of the multipole moments and polarizability of the target.

In an earlier paper (Danby and Tennyson 1990b, hereafter referred to as I) we discussed the implementation of an R-matrix program package generalized to deal with positron–diatom collisions. The most important modifications occur in the construction of the Hamiltonian matrix elements between mixed electron–positron configurations in the internal region. For positron collisions, bound–free exchange is absent and polarization–correlation effects are more pronounced due to the ability of the positron to enter occupied molecular spin orbitals. We can therefore study and test *ab initio* models for the treatment of polarization and correlation without the complication of the exchange interaction which plays such an important role in electron scattering. Furthermore, the opposing signs of the static and polarization potentials, and the resulting cancellation, impose more exacting requirements on the solution of the Schrödinger equation both inside and beyond the R-matrix sphere.

0953-4075/91/153517+13$03.50

The interplay between projectile and nuclear motions, which must be taken into account for a treatment of vibrational excitation, is very different for electrons and positrons. The repulsive static interaction slows down an incident positron as it approaches the nuclei, leading, as we show below, to a cross section for vibrational excitation which is larger than that determined in the adiabatic nuclei picture.

While studies of positron scattering complement the larger body of electron work, an important motivation for the current project is the recent development of electrostatic traps capable of storing large numbers of positrons. In the apparatus of Surko *et al* (1986, 1989) these are slowed down by collisions with N_2, with vibrationally inelastic processes likely to play a leading role at energies below a few eV.

All positron–N_2 calculations reported to date have been concerned with vibrationally elastic collisions. While Mukherjee *et al* (1989, 1991) have performed a close-coupling study of rotationally inelastic e^+–N_2 collisions, remaining results are for total cross sections (equivalent, at the adiabatic level, to a sum over all final rotational states) with the N_2 nuclei frozen at their equilibrium geometry. By neglecting velocity-dependent effects and virtual positronium formation, Elza *et al* (1989) have calculated an *ab initio* polarization potential subsequently modified by a spherical cut-off function parametrized to obtain agreement with experimental cross sections. This work demonstrated the qualitative difference between the polarization–correlation interactions for positrons and electrons out to at least 5 a_0. Gibson (1990, 1991) has applied a 'distributed positron' model to treat correlation effects in e^+–H_2 scattering, the successful outcome of which should encourage analogous work on N_2. In all cases the polarization-correlation potentials are added to the static interaction (exactly that for e^- scattering, but with a sign change). Calculations on low-energy positron–molecule, including N_2, collisions have been reviewed by Armour (1988).

In the first application of the molecular R-matrix method to positron collisions, Tennyson (1986) treated the interaction at the (*ab initio*) configuration interaction (CI) level. Short range correlation was accounted for by allowing the positron to enter occupied and virtual molecular orbitals (MO) determined from an SCF calculation on the ground state of N_2. A similar calculation was also reported for H_2. Polarization configurations were formed from one-electron excitations of the target with the positron entering MO determined by the overall symmetry. These two-particle–one-hole states allow for short-range polarization. In follow-up calculations, Tennyson and Danby (1987) further added the asymptotic polarization potential in the region outside the R-matrix sphere, beyond 10 a_0. As expected, this had most influence on the total cross sections at the lowest scattering energies studied (0.01–0.09 Ryd), but disagreement with the experiment of Hoffman *et al* (1982) persisted in this range. This provided strong motivation for extending the calculation to include excited target pseudostates which have been shown to effectively account for longer-range polarization within the R-matrix sphere for electron–N_2 collisions (Gillan *et al* 1988).

In I, we pointed to a programming error which beset the R-matrix calculations (Danby and Tennyson 1988) prior to 1989. The results of corrected calculations on H_2 (Danby and Tennyson 1990b) and HF (Danby and Tennyson 1990a) appear elsewhere. In section 3, we include corrected cross sections which demonstrate that the treatment of polarization adopted earlier leads in fact to poor agreement with experiment (Hoffman *et al* 1982, Charlton *et al* 1983) at all energies below the thresholds for positronium formation (0.647 Ryd) and electronic excitation (0.632 Ryd). We also compare our fixed-nuclei eigenphase sums with the new Kohn variational calculation of Armour and Plummer (1991).

Prior to this, in section 2, we provide an outline of the molecular R-matrix method, with particular emphasis on the differences due to scattering by a positron. Additional problems are encountered when one moves on from fixed-nuclei calculations at the equilibrium geometry to consider vibrational excitation: a set of electronic structure calculations must be performed at several fixed geometries as a prelude to either an adiabatic (section 4) or non-adiabatic (section 5) treatment of nuclear motion. For a given total symmetry, the number and types of electron/positron configurations are held constant for all geometries as determined from convergence studies at equilibrium.

2. Theory

The current implementation of the molecular R-matrix method has been described by Gillan *et al* (1987) and Morgan (1990). The generalization to positron scattering is dealt with in I. For a fixed-nuclei calculation in the body frame (z axis parallel to the internuclear axis), the wavefunction of the electrons and positron inside the R-matrix sphere ($a = 10\ a_0$ in this work) is:

$$\Psi_k(\boldsymbol{x}_1, \ldots, \boldsymbol{x}_N, \boldsymbol{x}_{N+1}; R) = \sum_{ij} c_{ijk}(R)\Phi_i(\boldsymbol{x}_1, \ldots \boldsymbol{x}_N; R)\eta_j(\boldsymbol{r}_{N+1}; R)\beta(\sigma_{N+1}) + \sum_i d_{ik}\phi_i(\boldsymbol{x}_1, \ldots, \boldsymbol{x}_N; R)\phi'_i(\boldsymbol{r}_{N+1}; R)\beta(\sigma_{N+1}). \quad (1)$$

In the present work, the Φ_i represent the SCF ground state, X $^1\Sigma_g^+$, and dipole polarization pseudostates of $^1\Sigma_u^+$ and $^1\Pi_u$ symmetry constructed (by a CI calculation) from single excitations from selected target MO. These are expressed as a linear combination of the 22-function basis of nuclei-centred Slater-type orbitals (STO) described by Tennyson (1986). These STO were used for all geometries. In (1), the parametric dependence on internuclear geometry, R, is indicated explicitly.

The MO, η, representing the continuum positron, are constructed by numerically solving, subject to suitable boundary conditions, the Schrödinger equation for a central potential. This is taken here to be the isotropic part of the e^+–N_2 static interaction. Solutions with energy below 9 Ryd for the lowest 3 partial waves, ℓ, appropriate for each of the six symmetries studied (Σ_g^+, Σ_u^+, Π_u, Π_g, Δ_g and Δ_u), are retained. Continuum MO are then formed by orthogonalizing all such solutions to the short-range positron MO, ϕ'. These were taken to be the same as the target MO, i.e. obtained from an SCF calculation on the ground electronic state. A Schmidt orthogonalization to all the short-range MO of the same symmetry is preceded by a Lagrange orthogonalization (Tennyson *et al* 1987) of the continuum orbitals to the $1\sigma_g$, $1\sigma_u$ and $1\pi_u$ target MO. Generating continuum basis functions whose derivatives are zero on the R-matrix boundary obviates the need to introduce a Bloch operator into the Hamiltonian (Gillan *et al* 1987).

The ground state configurations in (1), where Φ_i is the SCF X $^1\Sigma_g^+$ state, correspond to a calculation with a static potential. In this case, corresponding short-range terms with $\phi_i = \Phi_i$ must be present in the second summation in (1) to relax the orthogonality imposed on the η. The off-centre nature of these *correlation* configurations also accounts for some of the higher partial waves omitted from the first summation, which are needed to converge the calculation at short range in the region

of the nuclei. The remaining terms in the second summation are *two-particle–one-hole polarization* configurations, with ϕ_i being singlet spin states consisting of single excitations of the target, and the positron occupying those ϕ_i' appropriate to the total (electrons and positron) symmetry under consideration. The strategy of adding polarization pseudostate configurations to the first summation was shown to significantly improve the resulting total fixed-nuclei cross sections for e^+–H_2 reported in I for energies up to at least 1 Ryd. For convenience we shall refer to this as *intermediate range polarization* to distinguish it from the *short-range polarization* provided for by the two-particle–one-hole configurations.

Following I, the matrix elements between the configurations in (1) of the electronic–positronic Hamiltonian are evaluated, with subsequent diagonalization yielding the eigenvalues (poles) and eigenvectors of the R-matrix. The effect of higher poles is allowed for by applying a Buttle correction (Buttle 1967, Shimamura 1978) to the diagonal R-matrix elements. The resulting spectral representation of the R-matrix, evaluated at the surface of the R-matrix sphere, provides the necessary boundary condition for the solution of the body frame fixed-nuclei differential equations (e.g. Morrison 1988) in the external region. An R-matrix propagator (Morgan 1984a) was used out to 80 a_0, at which point a Gailitis asymptotic expansion (Noble and Nesbet 1984) is used to facilitate the extraction of the K-matrix (and hence eigenphase sums) from the known scattering boundary conditions. The T-matrix, and hence the total cross section, is then readily obtained.

In order to treat vibrational excitation, the above procedure is repeated for a series of nuclear geometries. The observed absence of resonant scattering, in stark contrast to the case of e^-–N_2 (Morgan 1984b, Gillan *et al* 1987, 1988), encourages the application of the computationally convenient adiabatic theory of Chase (1956). The T-matrix for vibrational excitation is then given by averaging the fixed-nuclei T-matrices over initial and final vibrational states, θ_v:

$$T_{\ell v,\ell' v'} = \int \theta_v T_{\ell\ell'}(R)\theta_{v'}\,\mathrm{d}R. \tag{2}$$

For θ_v we use Morse oscillators corresponding to a potential of the form:

$$V(R) = E_0 + D_e\{1 - \exp[-\beta(R - R_e)]\}^2. \tag{3}$$

The values for the parameters (E_0, D_e, β, R_e), chosen to fit the computed SCF energies of N_2, are ($-108.972\,972 E_h$, $0.798 E_h$, $1.118\ a_0^{-1}$, $2.0291\ a_0$). The value of D_e is about twice the actual well depth of N_2, a reflection of the small anharmonicity of the internuclear potential in the relevant region of the minimum and of our use of the SCF approximation.

The failure of the adiabatic approximation near threshold has been well documented for electron–molecule collisions (Morrison *et al* 1984, Morrison 1988). It can partially be remedied by scaling the resulting cross sections by the ratio of the wavenumbers relative to final (v') and initial (v) states, $k_{v'}/k_v$. In this work results are obtained without any such modifications as we are largely concerned with energies away from threshold.

The vibrational R-matrix method of Schneider *et al* (1979) can in principle provide an exact treatment of nuclear motion, equivalent to a full close-coupling calculation. In this generalization, the R-matrix sphere becomes a hypersphere with radii corresponding to the scattering coordinate, r, and the internuclear radius, R. Physically,

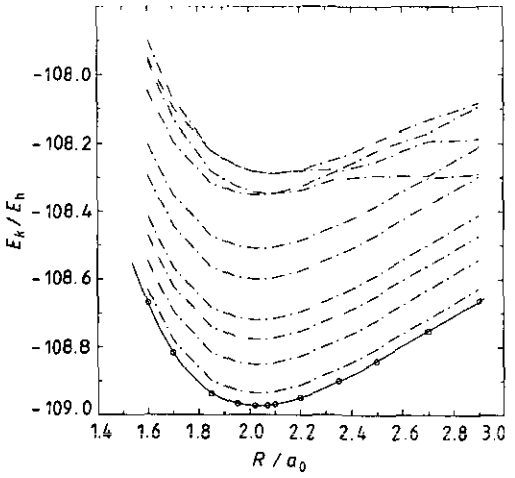

Figure 1. R-matrix pole positions with Π_u symmetry as a function of N_2 bond length (chain curve). The open circles represent our calculated N_2 SCF energies and the solid curve our Morse potential fit to them.

the fixed-nuclei R-matrix poles, $\epsilon(R)$, act as potential curves for the nuclear vibration. The presence of avoided crossings (figure 1), an indication of the rapid variation with R of the electronic–positronic wavefunction Ψ_k, necessitates an evaluation of matrix elements of the nuclear kinetic energy operator between e^-/e^+ configurations (Gillan *et al* 1987, Schneider 1983). However, the regular behaviour of the lowest poles in figure 1, which was found in the present work to be typical of all symmetries, encourages the application of a simplified treatment which should be valid at energies near threshold where the breakdown of the adiabatic nuclei approximation is most severe. For these poles we assume the e^-/e^+ wavefunction varies slowly with bond length so that the poles, E_K, and eigenvectors of the vibrational problem are obtained from the solution of (Gillan *et al* 1987):

$$\sum_{kv,k'v'} \left\langle \zeta_v \middle| \left(-\frac{1}{2\mu}\frac{\mathrm{d}^2}{\mathrm{d}R^2} + \epsilon_k(R) \right) \delta_{kk'} \middle| \zeta_{v'} \right\rangle \gamma_{Kvk}\gamma_{K'v'k'} = E_K \delta_{KK'} \tag{4}$$

where μ is the reduced mass of the nuclei and $\zeta_v(R)$ is a basis function, which in this work is a shifted Legendre polynomial (Morgan 1984b), representing the vibrational motion. The variational coefficients, γ, relate to the generalization of (1) to include nuclear motion:

$$\Theta_K = \sum_{kv} \Psi_k(\boldsymbol{x}_1, \ldots \boldsymbol{x}_N, \boldsymbol{x}_{N+1}; R)\zeta_v(R)\gamma_{Kvk}. \tag{5}$$

By including corrections due to the lowest poles, we relax the channel degeneracy aspect of the adiabatic approximation, known to be its most important flaw (Morrison *et al* 1991). An adiabatic average of the contribution to the R-matrix arising from the *higher* poles completes the inner region calculation.

In the outer region, we perform a full vibrational close-coupling calculation, evaluating the vibrational matrix elements of the quadrupole moment and dipole polarizability tensor. The results quoted in the present work, however, treat the outer

region polarizability as being geometry independent (since only the $R = 2.068\ a_0$ value appropriate to the present target basis set was available to us). Tests performed (at the adiabatic level) with the geometry-dependent polarizabilities of Morrison and Hay (1977) indicate that, while no significant error is introduced into the vibrationally elastic cross section, the $v = 0 \rightarrow 1$ cross section may be underestimated by 5% at 0.6 Ryd rising to over 20% below 0.1 Ryd.

3. Results

3.1. Nuclei fixed at equilibrium geometry

In order to test various models for e^+–N_2 scattering we performed a series of calculations with the target frozen at its equilibrium bondlength of $2.068\ a_0$. The calculations mainly focused on including short-, intermediate- and long-range polarization effects. Initially the calculations retained 17 target MO (set 1): 1–$5\sigma_g$, 1–$4\sigma_u$, 1–$3\pi_u$, 1–$3\pi_g, 1\delta_g$ and $1\delta_u$. They considered all symmetries up to Δ_u and retained the lowest three partial waves in each symmetry in the continuum basis.

The simplest model considered was the static (S). This included so called correlation configurations in the inner region but made no allowance for target polarization. The outer region potential was given only by an N_2 quadrupole of -0.8863 au determined from our SCF calculation. This may be compared with the experimental value of -1.04 (see, e.g., the tabulation of experimental and theoretical quadrupole moments and dipole polarizabilities given by Trail *et al* 1990). Short-range polarization effects were allowed for in the SP model (analogous to the SP4 calculation of Tennyson 1986) by allowing for two-particle–one-hole excitations of the target MO. All such excitations consistent with the total symmetry were retained in the calculation giving a total of (220, 221, 290, 291, 185, 186) polarization configurations for total symmetries $(\Sigma_g^+, \Sigma_u^+, \Pi_u, \Pi_g, \Delta_g, \Delta_u)$.

Intermediate polarization effects were studied by including polarized pseudostates in the calculation (Gillan *et al* 1988, Danby and Tennyson 1990b). In the SP10 model pseudostates were constructed by considering one-electron excitations from the $3\sigma_g$, $2\sigma_u$ and $1\pi_u$ MO to $4\sigma_g, 5\sigma_g, 3\sigma_u, 4\sigma_u, 2\pi_u, 1\pi_g, 1\delta_g, 1\delta_u$. The five states obtained by diagonalizing each of the resulting Hamiltonians with $^1\Sigma_u^+$ and $^1\Pi_u$ symmetry were used as pseudostates. In the SP10P model, polarization effects were included in the outer region potential by explicitly including the N_2 polarizability obtained by Gillan *et al* (1988) using the same SCF basis set as the present work ($\alpha_0 = 9.323$ au, $\alpha_2 = 4.197$ au). The comparable experimental values of α_0 and α_2 are, respectively, 11.744 au and 3.08 au (Trail *et al* 1990). This effect could also have been produced by explicitly retaining the pseudostates in the outer region, but this is computationally more expensive.

In our most sophisticated model, SP22P, we retained all 22 target MO (set 2: 1–$7\sigma_g$, 1–$7\sigma_u$, 1–$3\pi_u$, 1–$3\pi_g, 1\delta_g$ and $1\delta_u$) in the calculation. In this case the two-particle–one-hole excitations generated (473, 473, 483, 483, 263, 263) configurations for total symmetries $(\Sigma_g^+, \Sigma_u^+, \Pi_u, \Pi_g, \Delta_g, \Delta_u)$. Excitation from $3\sigma_g$, $2\sigma_u$ and $1\pi_u$ to 4–$7\sigma_g$, 3–$7\sigma_u$, 2–$3\pi_u$, 1–$3\pi_g, 1\delta_g, 1\delta_u$ gave $12\,^1\Sigma_u^+$ and $10\,^1\Pi_u$ target pseudostates. Again the polarizability of N_2 was included in the long-range potential.

Figure 2 compares eigenphase sums calculated for the models given above for the lowest three symmetries. It is notable that for all symmetries the eigenphase sum

increases monotonically as our treatment of target polarization effects is improved. Thus the static calculations with Σ_g^+ symmetry give only negative eigenphase sums as the potential is purely repulsive. Similarly the SP model gives negative Σ_g^+ eigenphase sums, except possibly at very low energies. However away from threshold the inclusion of short-range polarization effects leads to a significant increase in the eigenphase sums in all symmetries. The most significant increase in eigenphase sum, particularly at low energy, is obtained by including intermediate-range polarization effects by using pseudostates (SP10, SP10P, SP22P). With pseudostates included the Σ_g^+ eigenphase sum becomes clearly positive at low energy and the eigenphase sums in both Σ_u^+ and Π_u symmetry show pronounced peaks in the 0.1–0.2 Ryd region.

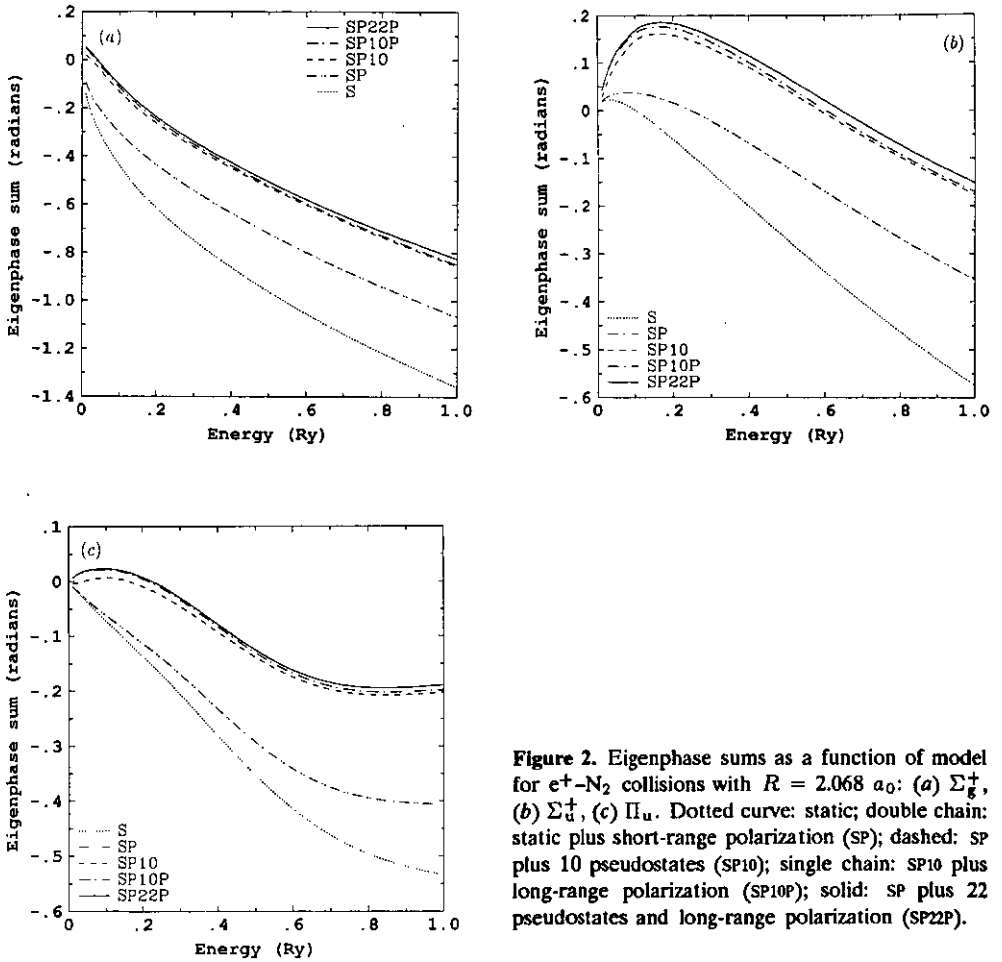

Figure 2. Eigenphase sums as a function of model for e^+–N_2 collisions with $R = 2.068\ a_0$: (*a*) Σ_g^+, (*b*) Σ_u^+, (*c*) Π_u. Dotted curve: static; double chain: static plus short-range polarization (SP); dashed: SP plus 10 pseudostates (SP10); single chain: SP10 plus long-range polarization (SP10P); solid: SP plus 22 pseudostates and long-range polarization (SP22P).

Table 1 compares our best results, the SP22P model, with the recent Kohn calculations of Armour and Plummer (1991). Given that the two calculations use very different techniques for including polarization effects, the level of agreement is perhaps surprising.

Figure 3 compares our cross sections, calculated by summing the contributions from all symmetries up to Δ_u, for various models with those measured by Hoffman *et al* (1982) and Charlton *et al* (1983). The measurements of Sueoka and Mori (1984),

Table 1. Eigenphase sums, in radians, for positron–N_2 (R_e = 2.068 a_0) scattering as a function of energy for our best model (SP22P). The results of Armour and Plummer (1991) are given for Σ_g^+ and Σ_u^+ symmetries as a comparison.

k^2/Ryd	Σ_g^+	Σ_g^+ [a]	Σ_u^+	Σ_u^+ [a]	Π_u	Π_g	Δ_g	Δ_u
0.01	0.054	0.060	0.042	0.050	0.006	0.007	0.000	0.002
0.04	0.001	0.028	0.108	0.117	0.018	0.022	0.004	0.007
0.09	−0.088	−0.056	0.163	0.200	0.023	0.042	0.011	0.013
0.16	−0.188	−0.145	0.186	0.235	0.017	0.067	0.018	0.021
0.25	−0.292	−0.374	0.173	0.227	−0.009	0.094	0.027	0.030
0.36	−0.395	−0.460	0.132	0.176	−0.059	0.117	0.035	0.040
0.49	−0.499	−0.577	0.074	0.113	−0.122	0.132	0.041	0.051
0.64	−0.608	−0.677	0.002	0.030	−0.173	0.141	0.044	0.061
0.81	−0.716	−0.782	−0.075	−0.061	−0.194	0.143	0.044	0.071
1.00	−0.824		−0.151		−0.189	0.134	0.042	0.080

[a] Armour and Plummer (1991).

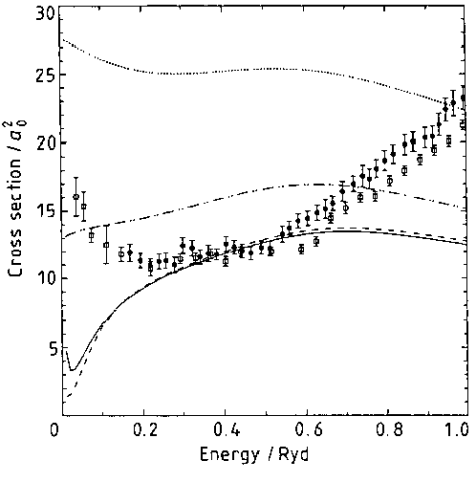

Figure 3. Total cross sections as a function of model for e^+–N_2 collisions with R = 2.068 a_0: Dotted curve: static; double chain: static plus short-range polarization (SP); dashed: SP plus 10 pseudostates (SP10); solid: SP plus 22 pseudostates and long-range polarization (SP22P). Experiment: □, Hoffman *et al* (1982); ●, Charlton *et al* (1983).

which are omitted from figure 3, are in agreement with the quoted experiments. Despite the inclusion of pseudostates, our best calculations significantly underestimate the low-energy cross section. Because of this our correct prediction of the cross section between 0.25 and 0.6 Ryd may be thought fortuitous. However, we note that similar behaviour was found for e^+–H_2 in I. It would appear that this energy region is less sensitive to short-range polarization effects; a view supported by the model calculations of Elza *et al* (1989). At higher energies we would not expect to reproduce the observed total cross section as our calculations included neither positronium formation nor N_2 electronic excitation.

It should be noted that the SP eigenphase sums (figure 2) and cross sections (figure 3) supersede those presented previously by Tennyson (1986) and Tennyson and Danby (1987).

3.2. Adiabatic vibrational motion

Whereas the equilibrium geometry calculations show a strong sensitivity to polarization effects, there is actually little difference between results obtained with our two most sophisticated models, SP10P and SP22P. We therefore adopted the SP10P model in our treatment of nuclear motion in both our adiabatic and non-adiabatic calculations. To this end the fixed-geometry calculations were repeated at a series of 12 N_2 internuclear separations: $R = 1.6, 1.7, 1.85, 1.95, 2.02, 2.068, 2.1, 2.2, 2.35, 2.5, 2.7$ and 2.9 a_0. These form a grid upon which the vibrational problem can be solved.

Analysis of the eigenphase sums and cross sections for these fixed-nuclei calculations shows a number of interesting trends. The most pronounced of these is that our predicted Ramsauer minimum moves to higher energy as the bond length increases. This means that at internuclear separations greater than 2.068 a_0 our low-energy cross sections increase rapidly with R, while the higher-energy cross sections drop slightly. The net effect is that the cross section computed for $R = 2.2$ a_0 (SP10P model) is in the best agreement with the $R = 2.068$ a_0 SP22P result of figure 3. This is probably a fortuitous consequence of the increase in polarizability of N_2 with R.

Another geometry-induced effect is the appearance of pseudo-resonances in our calculations at energies above 0.6 Ryd for calculations with large R. As our calculations neglect asymptotic channels leading to both positronium formation and electronically excited N_2, it is possible to get spurious resonance effects at energies above these thresholds (Burke *et al* 1981). This is particularly true when our polarization configurations mimic such things as 'virtual positronium' at short range. As both the positronium formation and electronic excitation thresholds decrease with increasing R, one would expect pseudo-resonance effects to be more apparent at large R. In practice the lowest such resonances occur just above 0.6 Ryd for $R = 2.9$ a_0, in both Σ_g^+ and Σ_u^+ symmetries. This is above the energy range of primary interest for vibrational excitation and therefore not a major cause for concern.

To obtain N_2 vibrational wavefunctions and corresponding energies, we fitted our SCF energies to a Morse potential (parameters given above). The high accuracy of this fit, see figure 1, suggests that this step does not introduce any significant errors.

Figure 4 presents adiabatic cross sections for vibrationally resolved elastic scattering and for excitation to the first vibrational state. In both cases the cross sections are given as a function of the number of symmetries included in the calculation. Clearly the elastic cross section is very well converged once symmetries higher than Π_u are included. The elastic cross section is very similar to the equivalent fixed geometry cross section given by figure 3.

Convergence with number of total symmetries included is slower for the vibrationally inelastic cross section. However our calculations appear to have converged with the inclusion of Δ_u. It is noteworthy that the predicted vibrational excitation cross sections are very small everywhere expect at threshold. In particular they are at least two orders of magnitude less than the corresponding elastic cross sections. This ratio is similar to that found in non-resonant electron collisions (e.g. Gillan *et al* 1987) although in this case both the elastic and inelastic cross sections are larger.

3.3. Non-adiabatic vibrational motion

To determine if the application of the adiabatic approximation for nuclear motion is significant for vibrational excitation of N_2 by positrons we performed non-adiabatic calculations using the theory of Schneider *et al* (1979). These calculations were

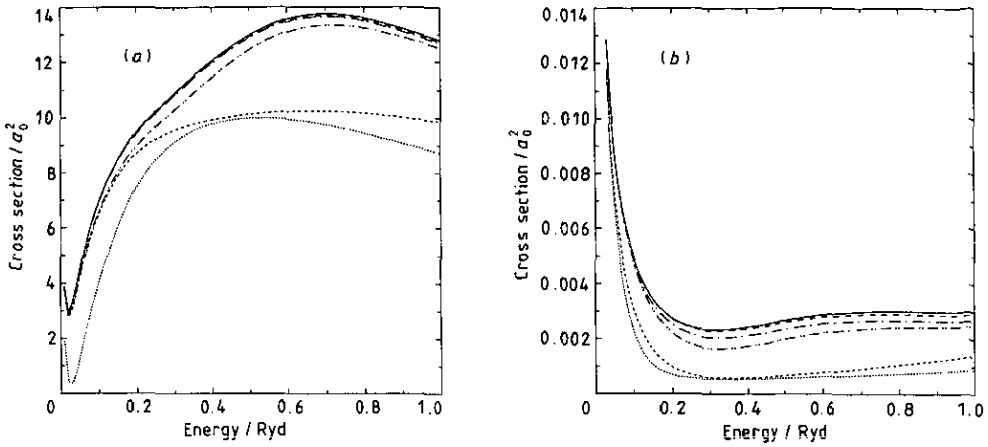

Figure 4. Cross sections as a function of total symmetries for adiabatic e^+–N_2 collisions: (*a*) $v = 0 \rightarrow 0$, (*b*) $v = 0 \rightarrow 1$. *Dotted curve:* Σ_g^+ *only; short dashed:* $\Sigma_g^+ + \Sigma_u^+$; double chain: same plus Π_u; single chain: same plus Π_g; long dash: same plus Δ_g; solid curve: sum of all symmetries from Σ_g^+ to Δ_u.

performed on the same grid of geometries as we used for the adiabatic calculations. As there are no resonances or pole crossings (see figure 1) in the energy region of interest ($k^2 \leqslant 0.6$ Ryd), we anticipated that such non-adiabatic effects should be minor.

A number of tests on convergence and stability of the non-adiabatic method were performed. These showed that the elastic $v = 0 \rightarrow 0$ and inelastic $v = 0 \rightarrow 1$ and $v = 0 \rightarrow 2$ cross sections were stable if eight vibrational states were explicitly retained in the calculation. These runs treated the lowest four or five R-matrix poles in each symmetry non-adiabatically and the higher poles by an adiabatic approximation to the R-matrix. The non-adiabatic cross sections were again checked for convergence with respect to the inclusion of total symmetries. Although the Σ_u^+ symmetry makes a larger contribution to the non-adiabatic than adiabatic cross section, the non-adiabatic cross sections are also well converged if all symmetries up to and including Δ_u are included in the sum.

Figure 5 compares integral cross sections obtained with both the adiabatic and non-adiabatic models. As expected the cross sections for $v = 0 \rightarrow 0$ are similar in both models. Near threshold, however, the non-adiabatic $v = 0 \rightarrow 1$ cross section is nearly double that of the adiabatic approximation.

We have also calculated cross sections for other vibrational transitions. Notably the $v = 0 \rightarrow 2$ are very significantly larger in the non-adiabatic than adiabatic calculations; although it should be stressed that in both cases the cross sections are very small compared to the single excitation ones. While we have no complete explanation for this difference it would appear that the adiabatic $v = 0 \rightarrow 2$ cross section is so small that non-adiabatic effects, which appear relatively small for larger cross sections, dominate. Above 0.4 Ryd, our calculations for this transition were unstable, which we attribute to the need to treat more poles non-adiabatically.

Figure 5(*a*), the vibrationally elastic cross section, also gives results for the fixed-nuclei calculation with $R = 2.068\ a_0$ for the same SP10P model. As the results

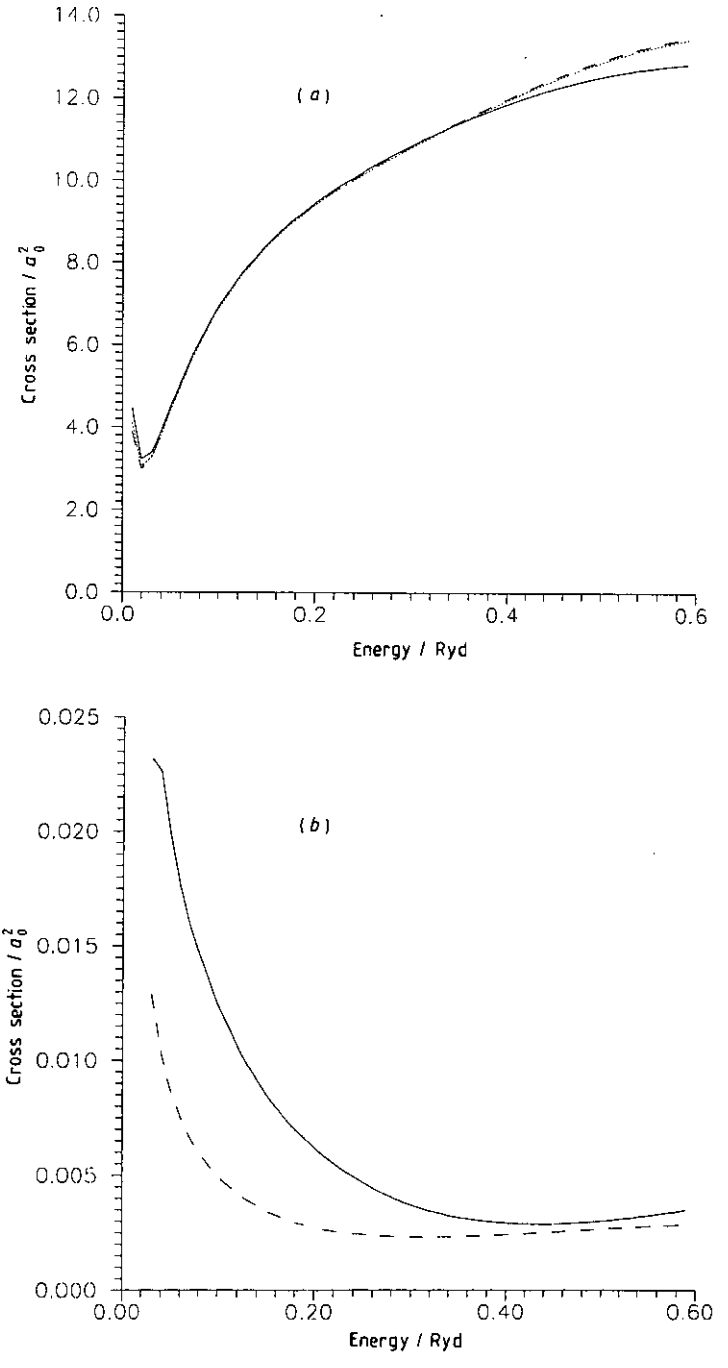

Figure 5. Cross sections for vibrationally resolved e^+–N_2 collisions: (*a*) $v = 0 \rightarrow 0$, (*b*) $v = 0 \rightarrow 1$. Dashed curve: adiabatic model; solid curve: non-adiabatic model; dotted curve: $R = 2.068\ a_0$ (*a* only).

with and without nuclear motion effects are very similar, this comparison confirms our supposition that the failure of our fixed nuclei calculation to reproduce the

experimental cross sections at low energy (see figure 3) is due to the incomplete representation of polarization effects in our calculation and not the absence of nuclear motion.

4. Conclusions

In this paper we report *ab initio* positron–nitrogen molecule collision calculations performed at a series of internuclear separations. These have been used to give not only elastic cross sections but also vibrationally inelastic cross sections calculated with both an adiabatic and non-adiabatic model. To our knowledge these are the first such *ab initio* non-adiabatic calculations for a e^+–molecule collision.

As with all *ab initio* studies of low-energy positron collisions, the adequate inclusion of electron–positron correlation or so called target polarization effects proved very difficult. Although we have done this more successfully than our previous work (Tennyson 1986, Tennyson and Danby 1987), our calculations are still unsatisfactory, at least at the lowest collision energies. It should be noted that the agreement with experiment above 0.1 Ryd obtained in the previous work was the spurious result of a programming error. It is, by contrast, plausible that the agreement obtained in the present work for energies above 0.2 Ryd comes from an energy-dependent sensitivity to the contributing polarization and correlation configurations.

There is no doubt that the inclusion of polarization effects in e^+ collision calculations is much more difficult than for the corresponding e^- calculation. Thus Gillan *et al* (1988) were able to reproduce the low-energy behaviour of the e^-–N_2 system with only two pseudostates. In this work we used up to 22 pseudostates for the analogous e^+ problem. However, in generating pseudostates we restricted ourselves to states whose symmetry was linked to the ground state by dipole transitions, i.e. states which could contribute to the long-range polarization potential. In this case these states were of $^1\Sigma_u^+$ and $^1\Pi_u$ symmetry. It is noteworthy that in atomic collision calculations a range of pseudostates is often used to represent polarization effects, irrespective of long-range considerations. We suggest such an approach and in particular the inclusion of pseudostates of $^1\Sigma_g^+$ symmetry may prove useful. This idea will be the subject of further work. We note that an alternative approach, the use of basis functions with explicit electron–positron distance dependence, has proved very successful for e^+–H_2 studies (Armour 1988). It may well be that only by using these so called Hylleraas functions can the low energy scattering behaviour be correctly reproduced.

A major motivating factor in the present calculations was the need for vibrational excitation cross sections for the e^+–N_2 system as this is a major means of cooling positrons below the N_2 electronic excitation threshold in positron traps (Surko *et al* 1989). Although we acknowledge the shortcomings of our calculations, we hope that the cross sections presented here will be of use for modelling these traps. To this end we note that our calculations do reproduce the observed elastic cross sections for energies in the region 0.25–0.6 Ryd.

Acknowledgments

We thank Lesley Morgan for helpful discussions during the course of this work, and Martin Plummer and Edward Armour for supplying their results prior to publication. This work was supported by Science and Engineering Research Council grant

GR/F/14550. GD also thanks Brian Elza, Andrew Feldt and Michael Morrison for useful discussions, and acknowledges financial support from NSF grant PHY-8805972. The calculations were performed on the Cray X-MP48 at the Atlas Laboratory.

References

Armour E A G 1988 *Phys. Rep.* **169** 1–98
Armour E A G and Plummer M 1991 *J. Phys. B: At. Mol. Opt. Phys.* submitted
Burke P G, Berrington K A and Sukumar C V 1981 *J. Phys. B: At. Mol. Opt. Phys.* **14** 289–305
Buttle P J A 1967 *Phys. Rev.* **160** 719–29
Charlton M, Griffith T C, Heyland G R and Wright G L 1983 *J. Phys. B: At. Mol. Phys.* **16** 323–41
Chang E S and Fano U 1972 *Phys. Rev.* A **6** 173–185
Chase D M 1956 *Phys. Rev.* **104** 838–42
Danby G and Tennyson J 1988 *Phys. Rev. Lett.* **61** 2737–9
—— 1990a *Annihilation in Gases and Galaxies* ed R J Drachman (NASA CP-3058) pp 91–3
—— 1990b *J. Phys. B: At. Mol. Opt. Phys.* **23** 1005–16 (corrigendum 1990 **23** 2471S)
Elza B K, Gibson T L, Morrison M A and Saha B C 1989 *J. Phys. B: At. Mol. Opt. Phys.* **22** 113-30
Gibson T L 1990 *J. Phys. B: At. Mol. Opt. Phys.* **23** 767–76
—— 1991 to be published
Gillan C J, Nagy O, Burke P G, Morgan L A and Noble C J 1987 *J. Phys. B: At. Mol. Phys.* **20** 4585–603
Gillan C J, Noble C J and Burke P G 1988 *J. Phys. B: At. Mol. Opt. Phys.* **21** L53–9
—— 1990 *J. Phys. B: At. Mol. Opt. Phys.* **23** L407–13
Hoffman K R, Dababneh M S, Hsieh Y-F, Kauppila W E, Pol V, Smart J H and Stein T S 1982 *Phys. Rev.* A **34** 2798–808
Morgan L A 1984a *Comput. Phys. Commun.* **31** 419–22
—— 1984b *J. Phys. B: At. Mol. Phys.* **19** L439–45
—— 1990 *Proc. XVIth Int. Conf. on Physics of Electronic and Atomic Collisions* ed A Dalgarno, R S Freund, M S Lubell and T B Lucatorto (New York: Plenum) Invited Papers and Progress Reports pp 96–102
Morrison M A 1983 *Aust. J. Phys.* **36** 239–86
—— 1988 *Adv. At. Mol. Phys.* **24** 51–156
Morrison M A, Abdolsalami M and Elza B K 1991 *Phys. Rev.* A **43** 3440–59
Morrison M A, Feldt A N and Austin D 1984 *Phys. Rev.* A **29** 2518–40
Morrison M A and Hay P J 1977 *J. Phys. B: At. Mol. Phys.* **10** L647–52
Mukherjee T, Ghosh A S and Jain A 1991 *Phys. Rev.* A **43** 2538–41
Mukherjee T, Sur S and Ghosh A S 1989 *Z. Phys.* D **11** 147–51
Noble C J and Nesbet R K 1984 *Comput. Phys. Commun.* **33** 399–411
Schneider B I 1983 *Electron-Atom and Electron-Molecule Collisions* ed J Hinze (New York: Plenum) p121–33
Schneider B I, Le Dourneuf M and Burke P G 1979 *J. Phys. B: At. Mol. Opt. Phys.* **40** L365–69
Shimamura I 1978 *Electronic and Atomic Collisions* ed G Watel (Amsterdam: North-Holland) 213–30
Sueoka O and Mori S 1984 *J. Phys. Soc. Japan* **53** 2491–500
Surko C M, Leventhal M, Crane W S, Passner A, Wysocki F, Murphy T J, Strachan J and Rowan W L 1986 *Rev. Sci. Instrum.* **57** 1862–7
Surko C M, Leventhal M and Passner A 1989 *Phys. Rev. Lett.* **62** 901–4
Tennyson J 1986 *J. Phys. B: At. Mol. Phys.* **19** 4255–63
Tennyson J, Burke P G and Berrington K A 1987 *Comput. Phys. Commun.* **47** 207–16
Tennyson J and Danby G 1987 *Atomic Physics with Positrons* ed E A G Armour and J W Humberston (New York: Plenum) pp 111–21
Trail W K, Morrison M A, Isaacs W A and Saha B C 1990 *Phys. Rev.* A **41** 4868–78